Article ID:1673-2812(2018)05-0705-09

Aluminum-Doped Zinc Oxide Thin Films Synthesized by Atomic Layer Deposition for Photocatalysis

EDY Riyanto[1,2], HUANG Gaoshan[2], ZHAO Yuting[2], ZHANG Jing[3], SHI Jianjun[3], MEI Yongfeng[2]

(1. State Key Laboratory for Modification of Chemical Fibers and Polymer Materials, College of Materials Science and Engineering, Donghua University, Shanghai 201620, China; 2. Department of Materials Science, Fudan University, Shanghai 200433, China; 3. College of Science, Donghua University, Shanghai 201620, China)

【Abstract】 Zinc oxide (ZnO) and aluminum-doped ZnO (AZO) thin films were fabricated by atomic layer deposition using porous polyurethane as a sacrificial template. ZnO and AZO were firstly deposited onto the surface of polyurethane porous template followed by a calcination at 500℃ in oxygen atmosphere. Three-dimensionally semiconductor porous structures as a replica of the sacrificial porous template were thus achieved. After pulverizing, the porous structures were broken into small pieces, which were then employed as photocatalysts. With increasing Al doping, the optical band gaps and the photocatalytic performance increase correspondingly.

【Key words】 atomic layer deposition; Al-doped ZnO; photocatalysis

CLC number: TB34 Document code: A DOI: 10.14136/j.cnki.issn 1673-2812.2018.05.004

原子层沉积制备铝掺杂氧化锌纳米薄膜及其光催化特性

EDY Riyanto[1,2],黄高山[2],赵宇婷[2],张 菁[3],石建军[3],梅永丰[2]

(1. 东华大学材料科学与工程学院,纤维材料改性国家重点实验室,上海 201620; 2. 复旦大学材料科学系,上海 200433; 3. 东华大学理学院,上海 201620)

【摘 要】 采用原子层沉积技术和多孔聚氨酯牺牲模板制备了氧化锌(ZnO)和铝掺杂氧化锌(AZO)纳米薄膜并研究了其光催化性能。首先利用原子层沉积技术,将 ZnO 和 AZO 沉积到多孔聚氨酯模板上,然后在 500℃高温煅烧处理去掉牺牲模板,得到复制了多孔模板的氧化物纳米薄膜三维多孔结构。将该三维多孔结构压碎,得到片状纳米薄膜。实验结果表明,随着铝掺杂含量的提高,材料的带隙和光催化性能也相应提升。

【关键词】 原子层沉积; 铝掺杂氧化锌; 光催化

1 Introduction

Semiconductor photocatalysis has received intensive attention in environmental purification owing to its simplicity, mild reaction conditions, and low energy consumption[1-2]. Transition metal oxide semiconductors such as TiO_2, and ZnO have been extensively studied for applications in photocatalytic activity, lithium ion battery, chemical and biological sensors, and electronic devices[2-12]. ZnO has

Received date: 2017-03-20; Modified date: 2017-04-19

Foundation item: National Natural Science Foundation of China (51322201, 51475093); Science and Technology Commission of Shanghai Municipality (14JC1400200)

Biography: EDY Riyanto, male, Indonesia, candidate of PhD. E-mail: edyr_01@yahoo.co.id.

Corresponding author: HUANG Gaoshan, professor. E-mail: gshuang@fudan.edu.cn.

attracted considerable attention because of its low cost and non-toxic nature[1, 13-15]. TiO_2 is known to be the most active photocatalyst for organic oxidation. Some certain studies, however, have reported that ZnO exhibits a better activity in photocatalytic performance as compared with TiO_2[16-18]. The high photocatalytic efficiency of ZnO is attributed to its higher ability to generate H_2O_2, more active sites and higher surface reactivity than TiO_2[17,19]. However, it was claimed that ZnO as a photocatalyst has several drawbacks including low stability due to photocorrosion[1], the high recombination rate of photogenerated electron-hole pairs, and a low quantum yield in the photocatalytic reactions in aqueous solutions which have been obstructing commercialization of the photocatalytic materials [16]. Consequently, a growing interest is exhibiting in improving the photocatalytic activity of ZnO. The improvement ideas include morphological change in nano-scale, composites structure optimization, defect introduction, and doping with transition metal oxides[16,20-21]. Among them, Al-doped ZnO (AZO) has received considerable attention because of its unique physical and chemical properties and low costs[16,22-24].

In this study, Al doped ZnO thin films were explored in terms of materials preparation and their photocatalystic performance. In the exploration, the phase structure, energy band structure, electron conductive path and acceleration of electron movements caused by the doping were taken into considerations.

2 Experimental methods

2.1 Synthesis of oxide thin films

In this work, ZnO and AZO films were firstly prepared by atomic layered deposition (ALD) on porous polyurethane sacrificial template ($67 \times 20 \times 3mm^3$). In the ALD, diethyl zinc (DEZ) was used as the precursor of Zn and mixed with water (H_2O) as the reactants. Both DEZ and H_2O were exposed to the ALD reactor via computer-controlled valves with pulse and purge time of 50 ms and 30s, respectively. In the case of AZO, Al_2O_3 as a doped-layer was deposited within the same pulse and purge time. The Al source of the precursor is trimethyl aluminum (TMA). For all doping and no doping depositions, the ALD reactor temperature was set at 150℃, and the temperatures of the TMA, DEZ, and H_2O precursor bottles were set at 60℃, 45℃, and 50℃, respectively. The thickness of the oxide film was controlled by the number of ALD cycles. In order to fabricate AZO thin film, a single layer of Al_2O_3 was inserted between the ZnO cycles. Two AZO samples were fabricated. The structure of AZO1 is 5 loops of ZnO (40 cycles)/Al_2O_3(1 cycle), while the structure of AZO_2 is 10 loops of ZnO (20 cycles)/Al_2O_3 (1 cycle). To achieve catalyst materials, the deposited sponges were calcined at 500℃ in oxygen atmosphere. Thisproccess was able to form the three-dimensionally porous structures composed of many small thin films or flakes due to the polyurethane template was carbonized and reacts with oxygen to forms CO_2. Eventually a large amount of thin films (flakes) can be formed by manual pulverization of the three-dimensionally porous structures. Thin films were also deposited on quartz substrates for comparison.

2.2 Characterization

The thin films morphologies were imaged by scanning electron microscopy (SEM, Phenom world). The crystal structures of photocatalyst were tested by X-ray diffraction (XRD) on a D8 spectrometer of Advance Bruker AXS GMBH, using Cu Kα radiation with irradiations condition of 40kV and 40mA. X-ray photoelectron spectroscopy (XPS) experiments were carried out on a RBD upgraded PHI-5000C ESCA system (Perkin Elmer) with Mg Kα radiation and the X-ray anode was run at 150W. Optical properties of ZnO and AZO thin films on quartz glass substrate were evaluated by UV-Vis spectrophotometer (Shimadzu UV-2550 spectrometer).

2.3 Photocatalytic measurement

Photocatalytic performance of ZnO and AZO were measured by photodegradation of MO solution using UV-Vis spectrophotometer. The ZnO-based thin films with the weight of 0.0125g were placed in 50mL MO solution with an initial concentration of 10mg/L, which was kept in the dark for 30min to

achieve the adsorption equilibrium, and then illuminated under the UV light irradiation of 200-W xenon lamp (Lanpu, China) with the distance of 50cm from the MO solution. The degradation of the MO was measured every 20min. The absorption intensity at the wavelength of 464nm is found to be the maximum absorption peak of MO, and the intensity was extracted to calculate the MO degradation.

3 Results and discussion

Figure 1 shows the fabrication schematic of ZnO and AZO thin films synthesized by ALD. In the process, the original porous polyurethane template (Fig. 1(a)) was deposited by ZnO or AZO with ~ 200 ALD cycles (Fig. 1(b)). To obtain pure photocatalyst, the deposited sponge was calcined in oxygen atmosphere at 500℃. Oxygen reacts with a carbonizable organic material to form CO_2 and flow out of the calcination chamber, which eventually causes the formation of three-dimensionally porous structures consisting of thin films (Fig. 1(c)). These structures were then pulverized manually to form powder/thin films (Fig. 1(d)). In the following photocatalytic applications, the thin films were employed as photocatalyst.

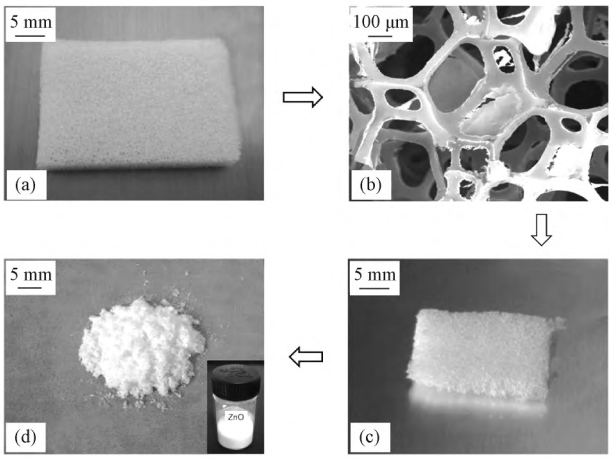

Fig. 1　Fabrication schematic of ZnO and AZO thin films synthesized by ALD. (a) Photo of porous polyurethane template. (b) SEM image of the deposited template before calcination. (c) Photo of the thin film after calcination, (d) Powder/thin film formed after pulverization of the structure shown in Fig. 1(c)

Figure 2 show the SEM images of zinc oxide-based thin films of (a) ZnO (200 cycles), Al-doped zinc oxide of (b) AZO1 ($ZnO(40)/Al_2O_3(1)$ 5 loops), and (c) AZO2 ($ZnO(20)/Al_2O_3(1)$ 10 loops). The original structure consists of ZnO or AZO porous structure as a replica of the porous polyurethane template, which then was transformed into thin films by pulverizing process (Fig. 2(a)~2(c)).

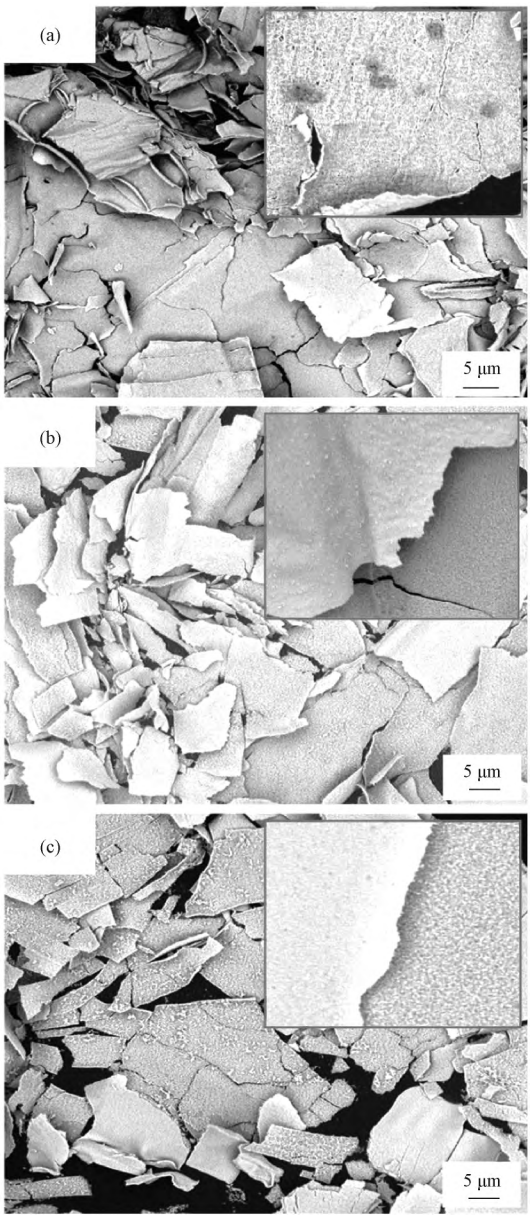

Fig. 2　SEM images of (a) ZnO (200cycle), (b) AZO1 ($ZnO(40)/Al_2O_3(1)$, 5 loops), (c) AZO2 ($ZnO(20)/Al_2O_3(1)$, 10 loops), calcined at 500℃

Figure 3 shows XRD patterns of ZnO and AZO thin films. It was shown that the strong and sharp peaks located at 2θ of 31.7, 34.4, and 36.2°, from (100), (002), and (101) planes, respectively of wurtzite structure of ZnO[1, 25-26]. Other peaks found at 2θ of 47.5, 56.6, 62.9, 66.4, 67.9, and 69.2°

correspond to (102), (110), (103), (200), (112), and (201) planes, respectively[1, 26-29]. It clearly shown that there is no additional peaks due to the aluminum insertion, which indicates that the fabricated AZO are in single phase condition[1, 16]. The doping of ZnO thin film by replacing Zn^{2+} with high valence atoms of Al^{3+} leads to stress formation in the crystalline structure and is known to be responsible for deterioration in ZnO crystallinity[30-33]. As a result, AZO thin films show weaker crystallinity with reducing peak intensities[34-37], as shown in Figs. 3(b)～3(c). The feasibility of Al incorporation into ZnO implies the ability to control the crystallinity as well as tailoring of the band gap[37]. It has been known that the excess of the Al solubility limit in ZnO leads to Formation of $ZnAl_2O_4$ with spinel-type structure[38-40], and indication of the formation of $ZnAl_2O_4$ crystalline phase can be selected as the criterion for solid solubility limit[30, 41-42]. The current experimental results indicate that the AZO formed is still in the range of solid solubility limit.

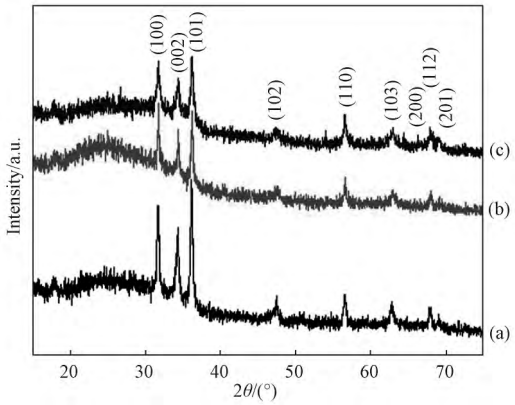

Fig. 3 XRD patterns of (a) ZnO (200 cycles) as well as AZO with various Al doping concentration of (b) AZO1 ($ZnO(40)/Al_2O_3(1)$, 5 loops), (c) AZO2 ($ZnO(20)/Al_2O_3(1)$, 10 loops)

Chemical compositions of Al-doped ZnO were measured by XPS. Figure 4 shows the XPS spectra of Zn, O, and Al of AZO thin films. It was shown in Fig. 4(a) that the Zn $2p^{3/2}$ and Zn $2p^{1/2}$ peaks are almost the same for the two AZO samples, and the peak positions are ascribed to wurtzite structure[16,43]. Figure 4(b) shows the Gaussian deconvoluted XPS O 1s spectra of AZO thin films. The two peaks of O1 and O2 can be assigned to the Zn-O bond, and the Al-O bond/adsorbed oxygen, respectively[16, 34, 44-46]. The slightly shift in the two samples can be attributed to the different chemical environment because the Zn-O bonds are affected by the substitution of Al atoms at Zn sites[47]. Fig. 4(c) shows the spectra of Al 2p of AZO thin films. It was shown that with increasing Al concentration the intensity of Al 2p peaks increases, and the Al atomic concentrations are calculated to be 1.3 % and 7.2 % for AZO1 and AZO2, respectively. The peak shifts to higher binding energy are believed to be due to more Al-O bonds[39].

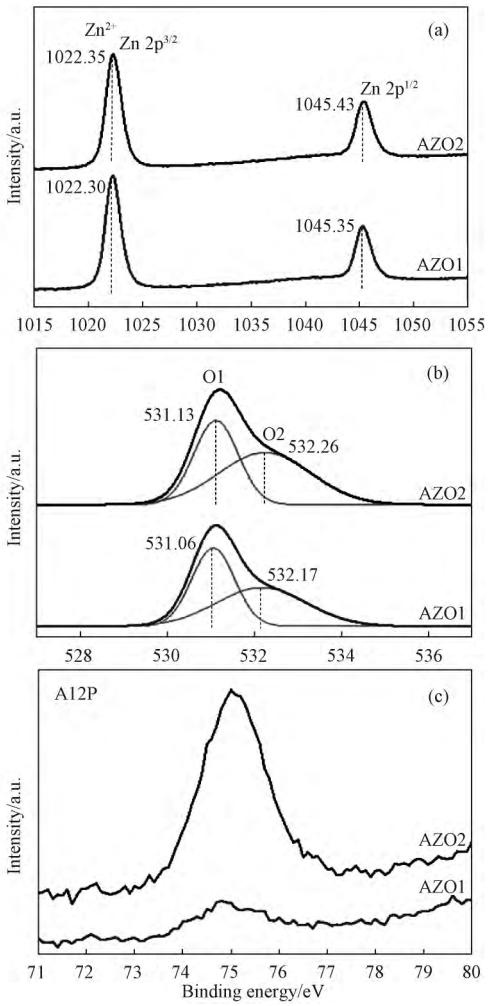

Fig. 4 XPS spectra of AZO1 ($ZnO(40)/Al_2O_3(1)$, 5 loops), and AZO2 ($ZnO(20)/Al_2O_3(1)$, 10 loops). (a) Zn 2p, (b) O 1s, and (c) Al 2p

Figure 5(a) shows the optical transmittance spectra of the ZnO and AZO thin films prepared on quartz substrates. It is shown that the optical transmittance of AZO thin films was slightly enhanced with increasing Al concentration, indicating that in the AZO, more facile electron transitions

exist to absorb photons[48-49]. The optical absorption coefficient, α, can be calculated using Lambert's equation[50-51]:

$$\alpha = \left(\frac{1}{t}\right)\ln\left(\frac{1}{T}\right)$$

where T is the optical transmittance and t is the thickness. The optical band gap (Eg) of ZnO and AZO can be evaluated by Tauc relation[47,52]:

$$\alpha h\nu = A\,(h\nu - Eg)^m$$

where A and $h\nu$ are the proportionality constant and incident photon energy, respectively and m is a constant with the value is equal to 1/2 for a direct band gap semiconductor. The direct band gaps of the oxides can be estimated from the curve of $(\alpha h\nu)^2 - (h\nu)$ by extrapolating the linear region of the curves to intercept the x-axis[47,53], as shown in Fig. 5(b). The estimated optical band gaps increase with increasing Al concentration as the values of the undoped ZnO, AZO1, and AZO2 are 3.13, 3.30, and 3.33eV, respectively. Here, the band gap of the ZnO (3.13eV) is in agreement to a reasonable extent with the accepted literature value of ~ 3.18 to 3.22eV[16,51,53-54]. The increase of the band gap with increasing Al doping is attributed to the Burstein-Moss effect, caused by an increase in free electron concentration due to Al doping[48,54-58]. ZnO thin films are naturally n-type oxide semiconductors due to natural electron donors generated by O vacancies and Zn interstitials[48]. The addition of donor Al^{3+} cations raises the Fermi level of the AZO thin films into the conduction band, causing complete degeneration, and therefore the absorption edge moves to higher energy[48,55].

Figure 6 (a) shows the photocatalytic performance of ZnO and AZO thin films annealed at 500℃ with MO solution used as a typical organic pollutant. The initial MO concentration is 10mg/L and ZnO or AZO photocatalysts concentration is 0.25mg/mL. It was shown that the presence of Al in ZnO gives a positive effect to the photocatalytic activities (Fig. 6(a)). AZO thin films with higher Al doping concentration (AZO2) has a wider optical band gap (Fig. 5(b)) and better photocatalytic performance than no and lower doping, e. g. ZnO (200 ALD cycles) and AZO1 in Figs. 6(a) and 6(b).

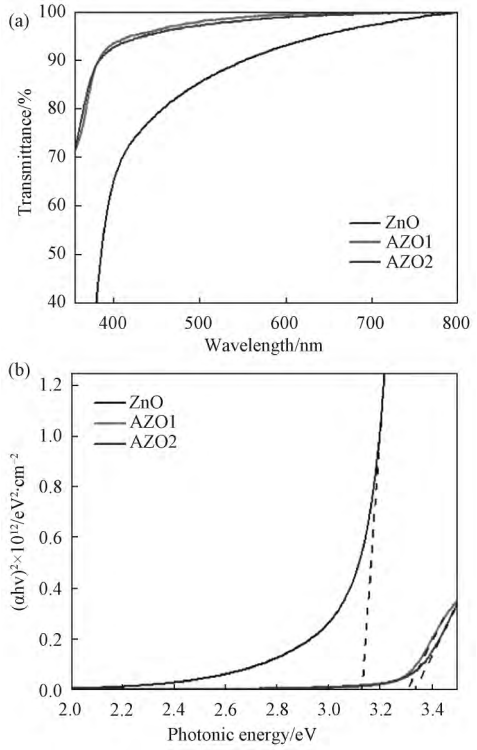

Fig. 5 (a) Optical transmittance spectra, and (b) plots of $(\alpha h\nu)^2$ against (hv) for ZnO (200 ALD cycles), AZO1 ($ZnO(40)/Al_2O_3(1)$, 5 loops), and AZO2 ($ZnO(20)/Al_2O_3(1)$, 10 loops)

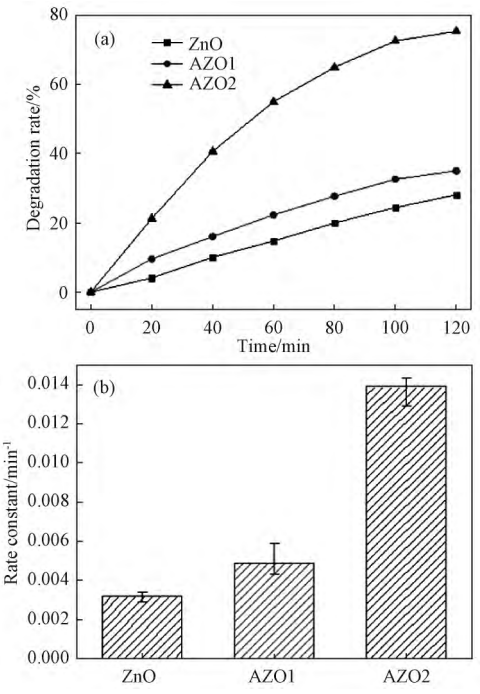

Fig. 6 (a) Photocatalytic performances of thin films: ZnO (200 ALD cycles), AZO1 ($ZnO(40)/Al_2O_3(1)$, 5 loops), AZO2 ($ZnO(20)/Al_2O_3(1)$, 10 loops). (b) Corresponding degradation rates, calculated from (a)

It can be explained as follows. The most important factor that can contribute to increase of photocatalytic activity is the presence of a high

electric conductive phases, which leads to an increase of the probability of the carriers reaching the photocatalyst/solution interface[19,59]. When a small amount of Al was introduced into the ZnO thin film, the one ionized Al^{3+} substitute for one Zn^{2+} giving one free electron to the conduction band for every Zn^{2+} site replaced by the Al^{3+}[53,60-61], which eventually increases the conductivity[53]. In the photocatalysis respect, Al doping increased the photocatalytic activity by accelerating the transfer of electrons to dissolved oxygen molecules[1]. The recombination of the photo-generated carriers was effectively suppressed leading to an increase in the photo-oxidation efficiency[1].

The photogenerated electrons and holes have been found to degrade many types of organic and inorganic pollutants which is possible to suggest that the electron-hole pair ($e^- - h^+$) is generated at the surface of thin films, leading to the formation of reactive oxidative hydroxide radicals. The process is described as follows[62]: when the ZnO/AZO is illuminated, the generation of electrons and holes begins (Eq (1)) and, as the semiconductor is immersed in a liquid medium, spontaneous adsorption of the molecules in a liquid occurs; then an electron is transferred to the acceptor molecule and the donor molecule gives an electron to the oxide [17]. The holes generate $OH^{\cdot}$ by reacting with the water molecules (Eq. (2)), and the O_2 molecule accepts an electron to form the super-oxide radical $O_2^{\cdot -}$ (Eq. (3)). These $O_2^{\cdot -}$ radicals act as strong oxidizing agents and they also contribute to the formation of hydrogen peroxide (Eqs. (4)—(7)) [17]. The formed radicals react with the dye molecule, disrupting it in its conjugated system which leads to the complete decomposition of the dye[17]. The presence of extra electrons contributes to the formation of $O_2^{\cdot -}$ radicals that accelerate the decomposition mechanism, reducing the dye discoloration time[17].

$$ZnO/AZO + h\nu \rightarrow e^{\square} + h^+ \quad (1)$$

$$H_2O + h^+ \rightarrow OH^{\cdot} + H^+ \quad (2)$$

$$O_2 + e^{\square} \rightarrow O_2^{\cdot -} \quad (3)$$

$$O_2^{\cdot -} + H^+ \rightarrow HO_2^{\cdot} \quad (4)$$

$$2HO_2^{\cdot} \rightarrow H_2O_2 + O_2 \quad (5)$$

$$H_2O_2 + O_2^{\cdot -} \rightarrow OH^{\cdot} + O_2 + OH^- \quad (6)$$

$$OH^{\cdot} + \text{dye} \rightarrow \text{dye mineralization} \quad (7)$$

4 Conclusion

ZnO and AZO thin films can be successfully deposited by ALD on porous polyurethane template. Calcination following the deposition makes the thin films form the three-dimensionally porous structures as a replica of the structure of original template. By pulverizing, the porous structures were broken into small pieces and form ZnO and AZO thin films. Experimental results show that the wurtzite crystal structure of ZnO can be maintained by Al doping, indicating a single phase structure. Furthermore, by presence and increasing of Al doping, the optical band gaps enlarges with the photocatalytic performance enhanced. The enlargement of optical band gap with increasing Al concentration is due to Al ions tending to occupy ZnO lattice planes, and consequently leading to the increase in transport path of charge carriers in ZnO lattice. The transport of photogenerated electrons to the outer systems will eventually be accelerated, resulting in high photocatalytic performance.

Reference

[1] M. Ahmad, E. Ahmed, Y. W. Zhang, et al. Preparation of Highly Efficient Al-Doped ZnO Photocatalyst by Combustion Synthesis[J]. Current Applied Physics, 2013, 13(4): 697～704.

[2] H. Kisch. Semiconductor Photocatalysis-Mechanistic and Synthetic Aspects [J]. Angewandte Chemie-International Edition, 2013, 52(3): 812～847.

[3] M. Batzill. Fundamental Aspects of Surface Engineering of Transition Metal Oxide Photocatalysts [J]. Energy & Environmental Science, 2011, 4(9): 3275～3286.

[4] X. B. Meng, X. Q. Yang, X. L. Sun. Emerging Applications of Atomic Layer Deposition for Lithium-Ion Battery Studies[J]. Advanced Materials, 2012, 24(27): 3589.

[5] J. S. Chen, X. W. Lou. Anatase TiO_2 Nanosheets: An Ideal Host Structure for Fast and Efficient Lithium Ensertion/Extraction[J]. Electrochemistry Communications, 2009, 11(12): 2332～2335.

[6] Y. Xu, E. M. Lotfabad, H. L. Wang, B. Farbod, Z. W. Xu, A. Kohandehghan, D. Mitlin. Nanocrystalline Anatase Tio_2: A New Anode Material for Rechargeable Sodium Ion Batteries[J]. Chemical Communications, 2013, 46(79): 8973～8975.

[7] X. Su, Q. L. Wu, X. Zhan, J. Wu, S. Y. Wei, Z. H. Guo. Advanced Titania Nanostructures and Composites for Lithium Ion Battery[J]. Journal of Materials Science, 2012, 47(6): 2519～2534.

[8] R. Edy, Y. T. Zhao, G. S. Huang, J. J. Shi, J. Zhang, A. A. Solovev, Y. F. Mei. Tio_2 Nanosheets Synthesized by Atomic Layer Deposition for Photocatalysis[J]. Progress in Natural Science-Materials International, 2016, 26(5): 493～497.

[9] P. M. Chassaing, F. Demangeot, V. Paillard, A. Zwick, N. Combe, C. Pages, M. L. Kahn, A. Maisonnat, B. Chaudret. Raman Study of E-2 and Surface Phonon in Zinc Oxide Nanoparticles Surrounded by Organic Molecules[J]. Applied Physics Letters, 2007, 91(5): 053108.

[10] S. Q. Pan, Y. T. Zhao, G. S. Huang, J. Wang, S. Baunanck, T. Gemming, M. L. Li, L. R. Zheng, O. G. Schmidt, Y. F. Mei. Highly Photocatalytic TiO_2 Interconnected Porous Powder Fabricated by Sponge-Templated Atomic Layer Deposition[J]. Nanotechnology, 2015, 26(36): 364001.

[11] Z. Wang, F. Mao, X. P. Huang, Y. P. Huang, S. Q. Feng, J. Yi, C. Y. Zhang, S. Liu, Preparation and Photocatalytic Activity of TiO_2/Graphene Composites[J]. Journal of Materials Science & Engineering, 2011, 29: 267～. 270.

[12] X. P. Yu, J. J. Fu, H. B. Wang, Alkali Precipitation Synthesis of Ce-Doped ZnO and Its Photocatalytic Activity[J]. Journal of Materials Science & Engineering, 2015, 33: 591～594.

[13] H. K. Park, J. Heo. Improved Efficiency of Aluminum Doping in ZnO Thin Films Grown by Atomic Layer Deposition[J]. Applied Surface Science, 2014, 309: 133～137.

[14] T. Tynell, M. Karppinen. Atomic Layer Deposition of ZnO: A Review[J]. Semiconductor Science and Technology, 2014, 29(4): 043001.

[15] A. Di Mauro, M. Cantarella, G. Nicotra, V. Privitera, G. Impellizzeri. Low Temperature Atomic Layer Deposition of Zno: Applications in Photocatalysis [J]. Applied Catalysis B-Environmental, 2016, 196: 68～76.

[16] H. J. Lee, J. H. Kim, S. S. Park, S. S. Hong, G. D. Lee. Degradation Kinetics for Photocatalytic Reaction of Methyl Orange Over Al-Doped ZnO Nanoparticles [J]. Journal of Industrial and Engineering Chemistry, 25: 199～206.

[17] M. Bizarro. High Photocatalytic Activity of ZnO And ZnO: Al Nanostructured Films Deposited by Spray Pyrolysis[J]. Applied Catalysis B-Environmental, 2010, 97(1): 198～203.

[18] M. Bizarro, A. Sánchez-Arzate, I. Garduno-Wilches, J. C. Alonso, A. Ortiz. Synthesis and Characterization of ZnO and ZnO: Al by Spray Pyrolysis with High Photocatalytic Properties [J]. Catalysis Today, 2011, 166(1): 129～134.

[19] R. Edy, G. S. Huang, Zhao Y, et al. Atomic Layer Deposition of TiO_2-Nanomembrane-Based Photocatalysts with Enhanced Performance[J]. AIP Advances, 2016, 6(11): 115113.

[20] P. Genevee, F. Donsanti, G. Renou, D. Lincot. Study of the Aluminum Doping of Zinc Oxide Films Prepared by Atomic Layer Deposition at Low Temperature [J]. Applied Surface Science, 2013, 264: 464～469.

[21] R. Murugan, T. Woods, P. Fleming, D. Sullivan, S. Ramakrishna, P. R. Babu. Synthesis and Photocatalytic Application of ZnO Nanoarrows[J]. Materials Letters, 2014, 128: 404～407.

[22] J. M. Huang, C. S. Ku, C. M. Lin, S. Y. Chen, H. Y. Lee. In Situ Al-Doped ZnO Films By Atomic Layer Deposition with an Interrupted Flow[J]. Materials Chemistry and Physics, 2015, 165: 245～252.

[23] M. Naddaf, M. Saad. Comparative Study of Structural and Visible Luminescence Properties of AZO Thin Film Deposited on GaAs and Porous GaAs Substrates[J]. Vacuum, 2015, 122: 36～42.

[24] P. Prepelita, V. Craciun, F. Garoi, A. Staicu. Effect of Annealing Treatment on the Structural and Optical Properties of AZO Samples[J]. Applied Surface Science, 2015, 352: 23～27.

[25] R. F. Silva, M. E. D. Zaniquelli. Aluminium Doped Zinc Oxide Films: Formation Process and Optical Properties [J]. Journal of Non-Crystalline Solids, 1999, 247(1): 248～253.

[26] H. Q. Wang, C. H. Li, H. G. Zhao, J. R. Liu. Preparation of Nano-Sized Flower-Like ZnO Bunches by a Direct Precipitation Method[J]. Advanced Powder Technology, 2013, 24(3): 599～604.

[27] P. S. Kumar, P. Paik, A. D. Raj, D. Mangalaraj, D. Nataraj, A. Gedanken, S. Ramakrishna. Biodegradability Study and pH Influence on Growth and Orientation of ZnO Nanorods via Aqueous Solution Process [J]. Applied Surface Science, 2012, 258(18): 6765～6771.

[28] H. Q. Wang, C. H. Li, H. G. Zhao, R. Lu, J. R. Liu. Synthesis, Characterization and Electrical Conductivity of ZnO with Different Morphologies [J]. Powder Technology, 2013, 239: 266～271.

[29] H. Y. Wu, M. L. Qin, A. M. Chu, Z. Q. Cao, P. Q. Chen, Y. Liu, X. H. Qu. Effect of Urea on The Synthesis of Al-Doped ZnO Nanoparticle and Its Adsorptive Properties for Organic Pollutants[J]. Materials Research Bulletin, 2016, 75: 78～82.

[30] B. Efafi, M. S. Ghamsari, M. A. Aberoumand, M. H. M. Ara, A. H. S. Ghamsari, H. H. Rad. Aluminum Doped ZnO Sol-Gel Derived Nanocrystals: Raman Spectroscopy and Solid Solubility Characterization [J]. Physica Status Solidi A-Applications and Materials Science, 2014, 211(10): 2426～2430.

[31] M. Louhichi, S. Romdhane, A. Fkiri, L. S. Smiri, H. Bouchriha. Structural and Photoluminescence Properties of Al-Doped Zinc Oxide Nanoparticles Synthesized in Polyol [J]. Applied Surface Science, 2015, 356: 998～1004.

[32] M. Moret, A. Abou Chaaya, M. Bechelany, P. Miele, Y. Robin, O. Briot. Atomic layer Deposition of Zinc Oxide For Solar Cell Applications[J]. Superlattices and Microstructures, 2014, 75: 477～484.

[33] S. Kahraman, H. M. Çakmak, S. Çetinkaya, F. Bayansal, H. A. Cetinkara, H. S. Guder. Characteristics of ZnO Thin Films

Doped by Various Elements[J]. Journal of Crystal Growth, 2013, 363: 86～92.

[34] X. Qian, Y. Q. Cao, B. L. Guo, H. F. Zhai, A. D. Li. Atomic Layer Deposition of Al-Doped ZnO Films Using Aluminum Isopropoxide as the Al Precursor[J]. Chemical Vapor Deposition, 2013, 19(4-6): 180～185.

[35] T. Tynell, H. Yamauchi, M. Karppinen, R. Okzaki, I. Terasaki. Atomic Layer Deposition of Al-Doped ZnO Thin Films [J]. Journal of Vacuum Science & Technology A: Vacuum, Surfaces, and Films, 2013, 31(1): 01A109.

[36] S. S. Lo, D. Huang, C. H. Tu, C. H. Hou, C. C. Chen. Raman Scattering and Band-Gap Variations of Al-Doped ZnO Nanoparticles Synthesized by a Chemical Colloid Process[J]. Journal of Physics D: Applied Physics, 2009, 42(9): 095420.

[37] A. N. Mallika, A. RamachandraReddy, K. SowriBabu, K. V. Reddy. Synthesis and Optical Characterization of Aluminum Doped ZnO Nanoparticles[J]. Ceramics International, 2014, 40 (8): 12171～12177.

[38] H. Serier, M. Gaudon, M. Menetrier. Al-Doped ZnO Powdered Materials: Al Solubility Limit and IR Absorption Properties[J]. Solid State Sciences, 2009, 11(7): 1192～1197.

[39] F. L. Zhao, J. C. Dong, N. N. Zhao, J. Wu, D. D. Han, J. F. Kang, Y. Wang. Characteristics of Atomic Layer Deposited Transparent Aluminum-Doped Zinc Oxide Thin Films at Low Temperature[J]. Rare Metals, 2016, 35(7): 509～512.

[40] Y. C. Cheng. Effects of Post-Deposition Rapid Thermal Annealing on Aluminum-Doped ZnO Thin Films Grown by Atomic Layer Deposition[J]. Applied Surface Science, 2011, 258(1): 604～607.

[41] J. P. Wiff, Y. Kinemuchi, K. Watari. Hall Mobilities of Al- and Ga-Doped ZnO Polycrystals[J]. Materials Letters, 2009, 63 (28): 2470～2472.

[42] K. Shirouzu, T. Kawamoto, N. Enomoto, J. Hojo. Dissolution Behavior of Al and Formation Process of $ZnAl_2O_4$ Phases in Al_2O_3-Doped ZnO Sintered Bodies [J]. Japanese Journal of Applied Physics, 2010, 49(1R): 010201.

[43] Gan X.-W, Wang T, Wu H, Liu C. ZnO Deposited on Si (111) with Al_2O_3 Buffer Layer by Atomic Layer Deposition [J]. Vacuum, 2014, 107: 120～123.

[44] C. H. Ahn, S. Y. Lee, H. K. Cho. Influence of Growth Temperature On The Electrical And Structural Characteristics of Conductive Al-Doped ZnO Thin Films Grown by Atomic Layer Deposition[J]. Thin Solid Films, 2013, 545: 106～110.

[45] Y. Wu, P. M. Hermkens, B. W. H. van de Loo, H. C. M. Knoops, S. E. Potts, M. A. Verheijen, F. Roozeboom, W. M. M. Kessels. Electrical Transport And Al Doping Efficiency in Nanoscale ZnO Films Prepared by Atomic Layer Deposition [J]. Journal of Applied Physics, 2013, 114(2): 024308.

[46] T. Dhakal, D. Vanhart, R. Christian, A. Nandur, A. Sharma, C. R. Westgate. Growth Morphology and Electrical/ Optical Properties of Al-Doped ZnO Thin Films Grown by Atomic Layer Deposition[J]. Journal of Vacuum Science & Technology A: Vacuum, Surfaces, and Films, 2012, 30(2): 021202.

[47] A. Sreedhar, J. H. Kwon, J. Yi, J. S. Gwag. Improved Physical Properties of Al-Doped ZnO Thin Films Deposited by Unbalanced RF Magnetron Sputtering [J]. Ceramics International, 2016, 42(13): 14456～14462.

[48] Y. J. Choi, S. C. Gong, D. C. Johnson, S. Golledge, G. Y. Yeom, H. H. Park. Characteristics of the Electromagnetic Interference Shielding Effectiveness of Al-Doped ZnO Thin Films Deposited by Atomic Layer Deposition[J]. Applied Surface Science, 2013, 269: 92～97.

[49] S. L. Qu, Y. L. Song, H. F. Liu, Y. X. Wang, Y. C. Gao, S. T. Liu, X. R. Zhang, Y. L. Li, D. B. Zhu. A Theoretical and Experimental Study on Optical Limiting in Platinum Nanoparticles[J]. Optics Communications, 2002, 203(3): 283～288.

[50] A. A. Al-Ghamdi, O. A. Al-Hartomy, M. El Okr, A. M. Nawar, S. El-Gazzar, F. El-Tantawy, F. Yakuphanoglu. Semiconducting Properties of Al Doped ZnO Thin Films[J]. Spectrochimica Acta Part A: Molecular and Biomolecular Spectroscopy, 2014, 131: 512～517.

[51] Z. Laghfour, T. Ajjammouri, S. Aazou, S. Refki, D. V. Nesterenko, A. Rahmouni, M. Abd-Lefdil, A. Ulyashin, A. Slaoui, Z. Sekkat. Structural and Opto-Electrical Properties of Al Doped ZnO Sputtered Thin Films[J]. Journal of Materials Science: Materials in Electronics, 2015, 26(9): 6730～6735.

[52] N. Hirahara, B. Onwona-Agyeman, M. Nakao. Preparation of Al-Doped ZnO Thin Films as Transparent Conductive Substrate in Dye-Sensitized Solar Cell[J]. Thin Solid Films, 2012, 520 (6): 2123～2127.

[53] C. M. Muiva, T.. S Sathiaraj, K. Maabong. Effect of Doping Concentration on the Properties of Aluminium Doped Zinc Oxide Thin Films Prepared by Spray Pyrolysis for Transparent Electrode Applications[J]. Ceramics International, 2011, 37 (2): 555～560.

[54] O. Gurbuz, S. Guner. Role of Annealing Temperature on Electrical and Optical Properties of Al-doped ZnO Thin Films [J]. Ceramics International, 2015, 41(3): 3968～3974.

[55] V. Devi, M. Kumar, D. K. Shukla, R. J. Choudhary, D. M. Phase, R. Kumar, B. C. Joshi. Structural, Optical and Electronic Structure Studies of Al Doped Zno Thin Films[J]. Superlattices and Microstructures, 2015, 83: 431～438.

[56] H. Yuan, B. Luo, D. Yu, A. J. Chen, S. A. Campbell, W. L. Gladfelter. Atomic Layer Deposition of Al-Doped ZnO Films Using Ozone as the Oxygen Source: A Comparison of Two Methods to Deliver Aluminum[J]. Journal of Vacuum Science & Technology A: Vacuum, Surfaces, and Films, 2012, 30(1): 01A138.

[57] T. F. Wei, Y. L. Zhang, Y. Yang, R. Q. Tan, P. Cui, W. J. Song. Effects of $ZnAl_2O_4$ Segregation in High Temperature Sintered Al-Doped ZnO Sputtering Target on Optical and Electrical Properties of Deposited Thin Films[J]. Surface and Coatings Technology, 2013, 221: 201～206.

(下转第 719 页)

4 结 论

1. 铝钢复合板在 600℃退火保温 30min 后，钢层晶粒由明显的纤维状加工组织变为细的等轴再结晶组织，当退火保温时间达到 240min 时，界面无金属间化合物生成。

2. 当退火温度为 610℃，保温时间为 30min 时，界面出现了不连续的金属间化合物，厚度约为 3～5μm。且随着温度升高和保温时间的延长，界面金属间化合物逐渐增厚。当界面金属间化合物的厚度超过 9.067μm 时，其界面结合性能显著降低。

3. 铝钢复合界面金属间化合物的生长规律符合抛物线特性。由于 Si 元素的扩散影响，金属间化合物的生长激活能为 Q＝328.723kJ/mol。铝钢界面金属间化合物的厚度与退火工艺(温度与时间)的关系满足 $X=5.55\times10^{6}\times\exp[-328723/(RT)\times t]^{1/2}$。

参 考 文 献

[1] 周德敬，尹林，等. 轧制复合铝/不锈钢界面金属间化合物的生长动力学[J]. 中国有色金属学报，2012，22(9)：2461～2469.

[2] 张小军，赵嘉莹，刘慧，周德敬. 退火对铝钢冷轧复合板组织和性能的影响[J]. 金属热处理，2014，7(39)：93～95.

[3] 王平，谢佩佩. 钢-铝轧制复合界面化合物的抑制机理[J]. 中国有色金属学报，2010，20(1)：284～289.

[4] 宋群玲，孙勇，范启印. 钢-铝轧制复合界面生成化合物的热力学计算及分析[J]. 材料热处理技术，2012，10(41)：114～117.

[5] 周德敬，尹林，等. Si 含量对轧制复合铝钢层状复合材料界面化合物组织形貌的影响[J]. 金属热处理，2014，1(39)：42～48.

[6] Vikas Jindal，V. C. Srivastava. Growth of Intermetallic Layer at Roll Bonded IF-steel/aluminum Interface [J]. Journal of Materials Processing Technology，2008，195：88～93.

[7] A. Bouayad，Ch. Gerometta，A. Belkebir，A. AmbarIi. Kinetic Interactions Between Solid Iron and Molten Aluminium [J]. Materials Science and Engineering A，2003，363：53～61.

[8] Shigeaki Kobayashi，Takao Yakou. Control of Intermetallic Compound Layers at Interface Between Steel and Aluminum by Diffusion-treatment[J]. Materials Science and Engineering A，2002，338：44～53.

[9] Wei-Jen Cheng，Chaur-Jeng Wang. Growth of Intermetallic Layer in the Aluminide Mild Steel During Hot-dipping [J]. Surface & Coatings Technology，2009，204：824～82.

[10] M. Yllmaz，M. Col，M. Acet. Interface Properties of Aluminum/steel Friction-welded Components [J]. Materials Characterization，2003，49：421～429.

[11] 吴铭方，司乃潮，王敬，王凤江. 铁铝扩散钎焊偶界面反应层生长机理分析[J]. 焊接学报，2011，32(5)：29～33.

[12] D. Naoi，M. Kajihara. Growth Behavior of Fe_2Al_5 During Reactive Diffusion Between Fe and Al at Solid-state Temperatures[J]. Materials Science and Engineering A，2007，459：375～382.

[13] T. Maitra，S. P. Gupta. Intermetallic Compound Formation in Fe-Al-Si Ternary System：Part II [J]. Materials Characterization，2003，49：293～311.

[14] Stanislaw Jozwiak，Krzysztof Karczewski，et al. Kinetics of Reactions in FeAl Synthesis Studied by the DTA Technique and JMA Model[J]. Intermetallics，2010，18：1332～1337.

[15] 曾祥勇，李龙，周德敬. 轧制复合铝-铝-钢界面金属间化合物生长动力学[J]. 金属热处理，2015，10(40)：22～28.

[16] S. P. Gupta. Intermetallic Compound Formation in Fe-Al-Si Ternary System：Part I[J]. Materials Characterization，2003，49：269～291.

[17] Fu-cheng YIN，Man-xiu ZHAO，et al. Effect of Si on Growth kinetics of Intermetallic Compounds During Reaction Between Solid Iron and Molten Aluminum [J]. Transactions of Nonferrous Metals Society of China，2013，23：556～561.

[18] Bo Wu，Long Li，et al. Effect of surface nitriding treatment in a steel plate on the interfacial bonding strength of the aluminum/steel clad sheets by the cold roll bonding process[J]. Materials Science and Engineering A.，2017，682：270～278.

[19] A Yahiro，T Masui，et al. Development of Nonferrous Clad Plate and Sheet by Warm Rolling with Different Temperature of Materials[J]. Isij International，1991，31(6)：647～654.

[20] Tomohiro Sasaki，Takao Yakou. Features of Intermetallic Compounds in Aluminized Steels Formed using Aluminum Foil [J]. Surface & Coatings Technology，2006，201：2131～2139.

[21] Qian WANG，Xue-song LENG，Tian-hao YANG，Jiu-chun YAN. Effects of Fe-Al Intermetallic Compounds on Interfacial Bonding of Clad Materials [J]. Transactions of Nonferrous Metals Society of China，2014，24：279～284.

(上接第 712 页)

[58] Q. Q. Hou，F. J Meng，J. M. Sun. Electrical and Optical Properties of Al-Doped ZnO And $ZnAl_2O_4$ Films Prepared by Atomic Layer Deposition[J]. Nanoscale research letters，2013，8(1)：144.

[59] E. García-Ramírez，M. Mondragon-Chaparro，O. Zelaya-Angel. Band Gap Coupling in Photocatalytic Activity in ZnO-TiO_2 Thin Films[J]. Applied Physics A，2012，108(2)：291～297.

[60] A. El Hichou，S. Diliberto，N. Stein. Influence of the Aluminum Incorporation on the Properties of Electrodeposited ZnO Thin Films[J]. Surface and Coatings Technology，2015，270：236～242.

[61] K. Ravichandran，N. J. Begum，S. Snega，B. Sakthivel. Properties of Sprayed Aluminum-Doped Zinc Oxide Films—A Review[J]. Materials and Manufacturing Processes，2016，31(11)：1411～1423.

[62] S. S. M. Hassan，W. I. M. El Azab，H. R. Ali，M. S. M. Mansour. Green Synthesis and Characterization of ZnO Nanoparticles for Photocatalytic Degradation of Anthracene[J]. Advances in Natural Sciences：Nanoscience and Nanotechnology，2015，6(4)：045012.